

1 Article

2 Effects of Powder Phase Properties on Pb(Zr, 3 Ti)O₃/Pb(Zr, Ti)O₃ Sol-Gel Composites

4 Makiko Kobayashi ^{1,*}, Hiroto Makino ² and Kei Nakatsuma ¹5 ¹ Faculty of Advanced Science and Technology, Kumamoto University, Kumamoto 860-8555, Japan;
6 e-mail@e-mail.com7 ² Graduate School of Science and Technology, Kumamoto University, Kumamoto 860-8555, Japan;
8 e-mail@e-mail.com9 * Correspondence: kobayashi@cs.kumamoto-u.ac.jp; Tel.: +81-96-342-3628

10

11 **Abstract:** The effects of the dielectric constant of the powder phase on lead zirconate titanate
12 (PZT)/PZT sol-gel composite films were investigated to tailor their electrical properties. Three
13 types of PZT powders were used to fabricate three different PZT/PZT sol-gel composite films. The
14 PZT powders had the same electromechanical coupling coefficient but different relative dielectric
15 constants. The PZT/PZT films were fabricated on a 3 mm-thick titanium substrate using an
16 automatic spray coating system, and their properties were investigated. The relative dielectric
17 constants of the PZT/PZT films were successfully controlled by tailoring the properties of the PZT
18 powder phase. However, the piezoelectric constants showed a tendency different to those of the
19 raw powders, because of the poor poling degree. This was overcome by conducting poling at a
20 high temperature.

21 **Keywords:** piezoelectric material; dielectric constant; piezoelectric constant

22

23

1. Introduction

24 Sol-gel composite materials have been developed to fabricate thick films without cracks [1].
25 The thick porous films have helped realize ultrasonic transducers with a relatively low center
26 frequency (in the range of 2–20 MHz); such transducers are suitable for non-destructive testing
27 (NDT) applications. Owing to the porosity of sol-gel composite films, ultrasonic transducers
28 fabricated using the sol-gel spray technique exhibit high-temperature durability, curved surface
29 applicability, reasonable signal strength, and high signal-to-noise ratio (SNR), in addition to the
30 suitable frequency range for NDT. Therefore, sol-gel composite-based ultrasonic transducers have a
31 good potential for industrial and medical applications [1–9].

32 Sol-gel composite materials are prepared using two raw materials: a sol-gel solution and a
33 piezoelectric powder. Each phase affects the overall properties of the composite. Various sol-gel
34 composites have been investigated. For example, sol-gel composites made of lead zirconate titanate
35 (PZT) powders and PZT sol-gel solution, namely the PZT/PZT composite, are expected to be useful
36 in many applications, as they exhibit a high sensitivity among sol-gel composites with poling facility
37 [1–4]. Although the relatively low maximum operating temperature (up to 200 °C) of PZT/PZT
38 composites is a disadvantage, many applications do not require operating temperatures above 85 °C,
39 and it is preferable to have a certain temperature stability [10–12]. Therefore, PZT/PZT composites
40 seem attractive for applications such as imaging and structural health monitoring.

41 The dielectric properties of PZT/PZT composites should be controlled to tailor the electrical
42 impedance depending on the application for a high electrical output power. It is difficult to obtain
43 reproducible results using the conventional manual spray coating technique. Therefore, an
44 automatic spray coating system has been developed for better reproducibility [13–15]. However,
45 controlling the dielectric properties of PZT/PZT composites remains challenging. Previous studies

46 have failed in this regard because of the particle size difference and top electrode quality difference
 47 The dielectric constant of PZT/PZT films was controlled through the PZT powder phase by
 48 maintaining the fabrication conditions as much as possible [16], though in the past report, ultrasonic
 49 measurement results were mainly discussed and there was no dielectric property discussion. In this
 50 paper, the difference in the electrical properties due to the PZT powder phase was evaluated.

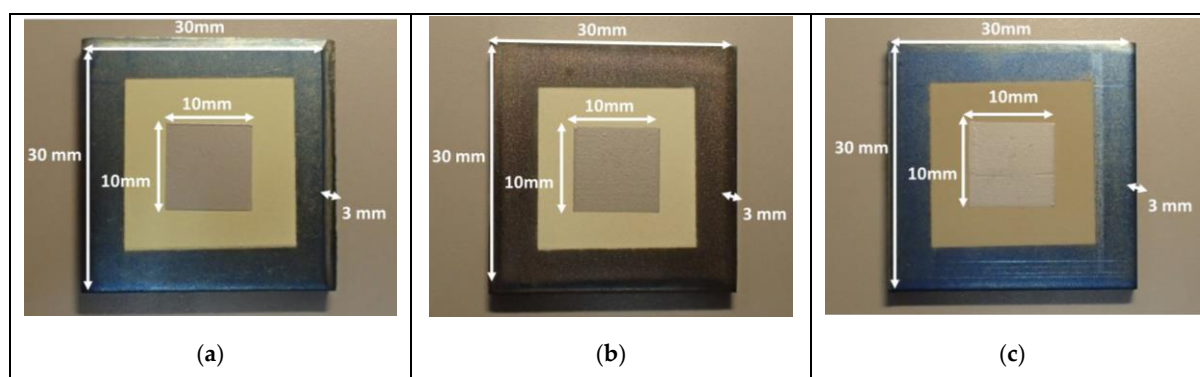
51 2. Sample Fabrication

52 Three types of PZT powders, namely HIZIRCO A(A), HIZIRCO L(L), and HIZIRCO
 53 MPT(MPT), were purchased from Hayashi Chemical Industry Co., Ltd. The particle size was
 54 specified as 0.6 μm . Table 1 lists the material properties of each powder.

55 **Table 1.** Properties of PZT powders.

Material property	HIZIRCO A	HIZIRCO L	HIZIRCO MPT
ϵ_r	5500	1800	1300
$k_{33}(\%)$	70	70	70
d_{33} ($\times 10^{-12}$ m/V)	660	400	290
g_{33} ($\times 10^{-4}$ Vm/N)	136	251	252

56 The piezoelectric constant (d_{33}) values of A, L, and MPT are high, medium, and low,
 57 respectively, whereas there is no significant difference in the electromechanical coupling coefficient
 58 k_{33} . The piezoelectric constant (g_{33}) values of L and MPT are higher than that of A. The three PZT
 59 powders were mixed in a laboratory-made PZT sol-gel solution. After ball milling, the mixture was
 60 sprayed onto titanium substrates with a thickness of 3 mm, a length of 30 mm, and a width of 30
 61 mm. An automatic spray coating system was used for the spray coating process to achieve a
 62 uniform coating in all cases. Subsequently, a thermal treatment, a drying process, and a firing
 63 process were conducted at 150 $^{\circ}\text{C}$ using a hot plate and at 650 $^{\circ}\text{C}$ using an electrical furnace. The
 64 spray coating and thermal treatment were repeated until the film reached the desired thickness. The
 65 film thickness was confirmed using a micrometer. After fabricating the films, poling was conducted
 66 through a positive corona discharge process to impart piezoelectricity for the sol-gel composite
 67 films. The output voltage was approximately 23 kV. It is difficult to measure the electrical field
 68 applied to the film, because electrical devices are easily destroyed by corona discharge. After poling,
 69 a 10-mm square silver top electrode was fabricated on each sample by a dispenser system to reduce
 70 the top electrode quality difference. Figure 1 shows the typical optical images of each sol-gel
 71 composite material. Except for the film color difference because of the piezoelectric powders, no
 72 significant difference was observed.
 73



74 **Figure 1.** (Color online) Optical images of (a) A/PZT (b) L/PZT, and (c) MPT/PZT films grown on 30
 75 mm \times 30 mm \times 3 mm titanium substrates.

76 3. Results and Discussion

77 The capacitance was measured using an LCR meter, and the relative dielectric constant ϵ_r was
78 calculated using the following equation:

$$79 \quad \epsilon_r = \frac{Cd}{\epsilon_0 A} \quad (1)$$

80 where C is the capacitance, d is the film thickness, ϵ_0 is the dielectric constant of vacuum, and A is
81 the area of the top electrode. The ϵ_r values of the A/PZT, L/PZT, and MPT/PZT films were found to
82 be 516, 465, and 326, respectively, as shown in Table 2, showing a similar tendency with those of the
83 piezoelectric powders; the difference was due to the porosity.

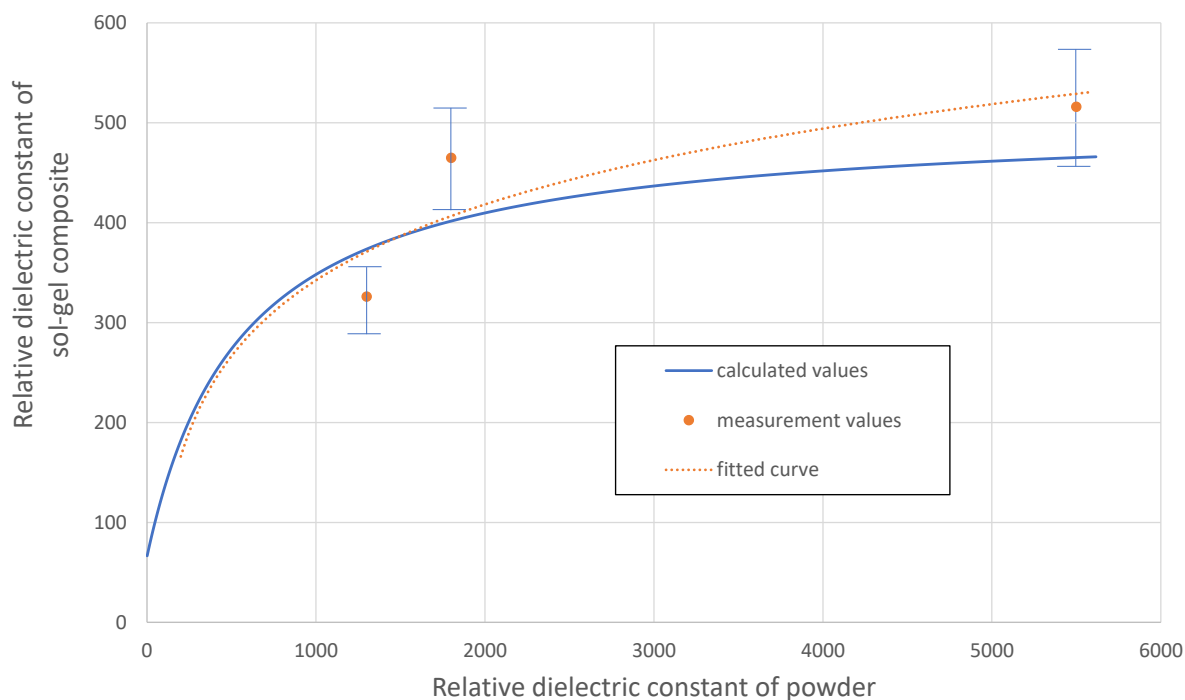
84 The average method [17] can be used for sol-gel composite properties, though the properties of
85 pure sol gel materials cannot be reliably measured. A cube model was proposed to determine the
86 properties of 0–3 composites using parallel and series equations, and in previous studies, the
87 theoretical values from the cube model showed reasonable agreement with the experimental values
88 concerning the dielectric constant of PZT/PZT films [1,3]. The dielectric constant of the PZT/PZT
89 sol-gel composites was calculated using the following equation:

$$90 \quad \epsilon_r = \frac{\epsilon_{r1}\epsilon_{r2}}{(\epsilon_{r2}-\epsilon_{r1})V_1^{-1/3} + \epsilon_{r1}V_1^{-2/3}} + \epsilon_{r2} \left(1 - V_1^{2/3}\right), \quad (2)$$

91 where ϵ_{r1} is the relative dielectric constant of the PZT powder phase, ϵ_{r2} is the relative dielectric
92 constant of the PZT sol-gel phase, and V_1 is the volume fraction of the PZT powder phase.

93 The results might not be accurate, as the phase of the pores was ignored. If spherical pores are
94 homogeneously dispersed throughout the PZT sol-gel phase, the PZT sol-gel phase can be
95 considered as another air/PZT 0–3 composite. Therefore, the relative dielectric constant of the
96 modified sol-gel phase was first calculated using Eq. (2), taking ϵ_{r1} as the relative dielectric
97 constant of the air phase, ϵ_{r2} as the relative dielectric constant of the PZT sol-gel phase, and V_1 as
98 the volume fraction of the air phase against the PZT sol-gel phase. The relative dielectric constant of
99 the modified sol-gel composite was then calculated using Eq. (2), taking ϵ_{r1} as the relative dielectric
100 constant of the PZT powder phase, ϵ_{r2} as the relative dielectric constant of the modified sol-gel
101 phase, and V_1 as the volume fraction of the PZT powder phase. Thus, with the double-cube model,
102 the effect of pores is considered, and the accuracy of the calculation can be improved. Figure 2 shows
103 the typical results. The solid line indicates the fitting curve derived from the three experimental
104 values, and the dashed line indicates the curve obtained using Eq. (2) (best fitting method). For the
105 best fitting method, the volume fraction of the air phase, the relative dielectric constant of the PZT
106 sol-gel phase, and molar ratio of the PZT powder to the PZT sol-gel were estimated to be 0.25, 400,
107 and 7:3, respectively. Figure 2 shows that the calculation results are in good agreement with the best
108 fitting results. However, the simulation results are not in good agreement with the experimental
109 results. Following are the possible reasons for the same: measurement errors of film thickness due to
110 surface roughness, measurement errors of capacitance due to the thick silver paste top electrode,

111 uncertainty in the volume fraction of the air phase, relative dielectric constant of the PZT sol-gel
 112 phase, and/or molar ratio of the PZT powder to the PZT sol-gel. However, the volume fraction of the
 113 air phase reasonably agreed with previous SEM cross-sectional measurement results. Owing to the
 114 automatic spray coating system, the surface roughness was within $\pm 5 \mu\text{m}$. This value is less than that
 115 realized when using the manual spray system, resulting in an efficient dielectric control, even
 116 though the error increases with the increase in the dielectric constant of the powder.



117
 118 **Figure 2.** (Color online) Typical relative dielectric constant calculation results of PZT/PZT
 119 films from the double-cube model considering the effect of pores, as a function of the
 120 relative dielectric constant of the powders.

121
 122 The piezoelectric constants were also measured and calculated. Table 2 lists the measured film
 123 properties. The piezoelectric constant of the L/PZT film is the highest, even though the piezoelectric
 124 constant of A is higher than that of L. This tendency was reproducibly observed, and as the dielectric
 125 constant of PZT sol-gel is much lower than those of bulk ceramics [18] (decreasing further as it
 126 becomes porous), the electrical field might not have been sufficiently applied to the PZT powders
 127 during the poling process when the dielectric constant of the PZT powder is too high. The
 128 piezoelectric constants of the PZT/PZT films showed a better agreement with those of the PZT
 129 powders because of the low dielectric constant. The piezoelectric constant of the A/PZT film can be
 130 improved by modifying the poling conditions. With the automatic spray coating system, 20 μm -thick
 131 PZT/PZT films were fabricated on 30 mm \times 30 mm \times 3 mm titanium substrates by poling at 150 $^{\circ}\text{C}$;
 132 the previous samples were poled at room temperature. Other poling conditions, such as the poling
 133 voltage and distance between the sample and the needle, were unchanged. Table 3 lists the results of
 134 the measured piezoelectric constant. The dielectric constant of the A/PZT film is comparable to that
 135 of the L/PZT film, thus proving our hypothesis. Poling is often conducted at a high temperature, e.g.,
 136 approximately half the Curie temperature, to achieve a sufficient poling degree, even though
 137 domain wall switching theory is still under investigation. The results might have been influenced by

138 the critical size reduction for nucleus formation during domain growth.

139 **Table 2.** Properties of PZT/PZT films with the top electrode fabricated using a dispenser.

Film property	A/PZT	L/PZT	MPT/PZT
Thickness (μm)	47	49	49
Capacitance (nF)	9.71	8.40	5.88
ϵ_r	516	465	326
	44.8	51.1	34.9
d_{33} ($\times 10^{-12}$ m/V)			
g_{33} ($\times 10^{-4}$ Vm/N)	98.2	124	121

140 **Table 3.** Properties of PZT/PZT films poled at high temperature.

Film property	A/PZT	L/PZT	MPT/PZT
Thickness (μm)	20	20	20
d_{33} ($\times 10^{-12}$ m/V)	24.4	24.0	17.8

141 4. Conclusions

142 Three types of PZT powders with different dielectric constants were used to fabricate PZT/PZT
 143 sol-gel composite films on a 3 mm-thick titanium substrate using an automatic spray coating system.
 144 The effects of powder phase properties on the fabricated films were investigated. The relative
 145 dielectric constants of the PZT/PZT films were successfully controlled by tailoring the properties of
 146 the PZT powder phase, showing a reasonable agreement with the simulated results obtained using
 147 the double-cube model considering the presence of air inside the films. The piezoelectric constant of
 148 the films was lower than expected when the dielectric constant of the PZT powder phase was too
 149 high. This was overcome by poling at a high temperature (instead of room temperature).

150 References

- 151 1. Barrow, D.A.; Petroff, T.E.; Tandon, R.P.; Sayer, M. Characterization of thick lead zirconate titanate films
 152 fabricated using a new sol gel based process. *J. Appl. Phys.* **1997**, *81*, 876.
- 153 2. Zhu, H.; Miao, J.; Wang, Z.; Zhao, C.; Zhu, W. Fabrication of ultrasonic arrays with 7 μm PZT thick films as
 154 ultrasonic emitter for object detection in air. *Sensors Actuators A: Phys.* **2005**, *123–124*, 614–619.
- 155 3. Bardaine, A.; Boy, P.; Belleville, P.; Acher, O.; Levassort, F. Influence of powder preparation process on
 156 piezoelectric properties of PZT sol-gel composite thick films. *J. Sol-Gel Sci. Technol.* **2008**, *48*, 135–142.
- 157 4. Zhu, B.P.; Wu, D.W.; Zhou, Q.F.; Shung, K.K. Lead zirconate titanate thick film with enhanced electrical
 158 properties for high frequency transducer applications *IEEE Inter. Ultrason. Symp. Proc.*, **2008**, p. 70.
- 159 5. Searfass, C.T.; Pheil, C.; Sinding, K.; Tittmann, B.R.; Baba, A.; Agrawal, D.K. Bismuth titanate fabricated by
 160 spray-on deposition and microwave sintering for high-temperature ultrasonic transducers *IEEE Trans.*
 161 *Ultrason. Ferroelect. Freq. Contr.*, **2016**, 139.
- 162 6. Searfass, C.T.; Baba, A.; Tittmann, B.R.; Agrawal, D.K. Fabrication and testing of microwave sintered
 163 sol-gel spray-on bismuth titanate-lithium niobate based piezoelectric composite for use as a high
 164 temperature ($>500^\circ\text{C}$) ultrasonic transducer. *AIP Conference Proceedings*, **2010**, *1211*, 1035.
- 165 7. Inoue, T.; Kobayashi, M. $\text{PbTiO}_3/\text{Pb}(\text{Zr},\text{Ti})\text{O}_3$ sol-gel composite for ultrasonic transducer applications. *Jpn.*
 166 *J. Appl. Phys.* **2014**, *53*, 07KC11.
- 167 8. Kimoto, K.; Matsumoto, M.; Kaneko, T.; Kobayashi, M. Sol-gel composite material characteristics caused
 168 by different dielectric constant sol-gel phases. *Jpn. J. Appl. Phys.* **2016**, *55*, 07KB04.

- 169 9. Yamamoto, T.; Kobayashi, M. CaBi₄Ti₄O₁₅-based lead-free sol-gel composites for high-temperature
170 application. *Jpn. J. Appl. Phys.* **2018**, *57*, 07LB16.
- 171 10. Mimura, M.; Tamazaki, D.; T. Yamane, T.; Kando, H. Improvement of temperature characteristics of
172 boundary acoustic wave resonators using multilayered electrodes., *Jpn. J. Appl. Phys.* 2012, *51*, 07GC13
173 (2012).
- 174 11. Nakase, R.; Nakata, K.; Matsukawa, M., Nondestructive evaluation of plane crack tip in a thin plate using
175 laser-induced pulse wave and symmetric Lamb wave. *Jpn. J. Appl. Phys.* 2012, *51*, 07GB16 (2012).
- 176 12. Takarada, J.; Wakatsuki, N.; Mizutani, K. Monolithic piezoelectric sensor for measurement of triaxial
177 forces applied to bridge by string vibration. *Jpn. J. Appl. Phys.* 2011, *50*, 07HC03 (2011).
- 178 13. Kiyota, Y.; Nakatsuma, K.; Kobayashi, M. Flexible ultrasonic transducers by automatic spray coating for
179 non-destructive testing. *Proc. IEEE Int. Ultrason. Symp.* **2017**, 17317793.
- 180 14. Kobayashi, M.; Kiyota, Y.; Nakatsuma, K. Sol-gel composite ultrasonic transducers made by automatic
181 spray system *Proc. The Sixth Japan-US NDT Symp.*, **2018**.
- 182 15. Kiyota, Y.; Nakatsuma, K.; Kobayashi, M. Effect of piezoelectric powder phase permittivity on Pb(Zr,
183 Ti)O₃/Pb(Zr, Ti)O₃ thin films *Proc. Symp. Ultrasonic Electronics*, **2017**, 3P1-6.
- 184 16. Kiyota, Y.; Makino, H.; Nakatsuma, K.; Kobayashi, M.; Piezoelectric powder permittivity effect of Pb(Zr,
185 Ti)O₃/Pb(Zr, Ti)O₃ *Proc. Symp. Ultrasonic Electronics*, **2018**, 2P1-11.
- 186 17. Banno, H.; Saito, S. Piezoelectric and dielectric properties of composites of synthetic rubber and PbTiO₃ or
187 PZT. *Jpn. J. Appl. Phys.* **1983**, *22*, 67.
- 188 18. Sayer, M.; Lukacs, M.; Olding, T.; Pang, G.; Zou, L.; Chen, Y. Piezoelectric films and coatings for device
189 purposes. *Materials Research Society Proc.*, **1998**, *541*, 599.